Breaking Elastic Field Symmetry with Substrate Vicinality

L. Persichetti, A. Sgarlata, M. Fanfoni, and A. Balzarotti

Dipartimento di Fisica, Università di Roma Tor Vergata, Via della Ricerca Scientifica,1-00133 Roma, Italy

(Received 4 November 2010; published 2 February 2011)

We present a novel approach to engineer the growth of strained epitaxial films based on tailoring the elastic-interaction potential between nanostructures with substrate vicinality. By modeling the island-island interaction energy surface within continuum elasticity theory, we find that its fourfold symmetry is broken at high miscuts, producing directions of reduced elastic-interaction energy. As a consequence, it is possible to direct the Ge island growth on highly misoriented Si(001) substrates towards desired pathways.

DOI: 10.1103/PhysRevLett.106.055503 PACS numbers: 81.10.Aj, 62.23.Eg, 68.35.bg, 68.37.Ef

Engineering the growth of strained epitaxial films is a fascinating perspective in modern nanoscale science. To this purpose, the challenge is to control the strain-relief mechanisms which play a key role in the growth of nanostructures. This can be done ''artificially,'' e.g., exploiting patterning surface features [1–3] or multilayered structures [4,5]. A conceptually different approach is the manipulation of heteroepitaxy through intrinsic properties of the substrate. To make this prospect feasible, one has to identify (1) distinct properties, which have impact on the growth process, and (2) a simple and reliable way of tuning them.

In strained-layer epitaxy, the nature of the elastic field is a crucial parameter by definition. Thus, tuning the elastic interactions between nanostructures could be appropriate to tailor the growth mode. Recently, we have shown that a fine shaping of Ge islands is possible on Si(001) by changing the miscut angle [6]. This offers a direct way to easily alter the elastic-interaction potential among islands, which strongly depends on the detailed island's shape.

In this Letter, we show that, breaking the isotropy of elastic interactions with miscut, it is possible to force the growth of Ge on Si(001) towards completely different pathways than on the flat substrate. Specifically, by modeling the island-island interaction energy surface for realistic 3D shapes, we find that the morphological anisotropy of islands at high miscuts [7,8] breaks the fourfold symmetry of elastic potential, producing directions of reduced elastic-interaction energy. This turns into a strong modification in the growth evolution, which is captured by the experiment.

Continuum elasticity theory implemented within a finite-element model is a powerful tool for simulating strain-related effects [9,10]. In the present work, this approach is used to compute the elastic-interaction energy between Ge islands both on the flat Si(001) surface and on a highly misoriented substrate. We focus on the large multifaceted Ge islands (the so-called ''domes'') [11–13], because their elastic field is particularly intense [14].

The strain components, ϵ_{ij}, in the system (interacting Ge domes + Si substrate) were determined using the finite-element simulation to solve the set of 3D equations of the linear elasticity for an elastic body at equilibrium which experiences a misfit strain in absence of volumetric and surface forces

$$\sigma_{ij,j} = 0, \qquad \epsilon_{ij} = (u_{i,j} + u_{j,i})/2, \qquad \sigma_{ij} = C_{ijkl}(\epsilon_{kl} - \epsilon_0 \delta_{kl}), \tag{1}$$

where σ_{ij} are the stress components, C_{ijkl} is the stiffness tensor, and ϵ_0 is 4% in the islands and zero in the substrate [15]. The values of the anisotropic stiffness tensor of Ge and Si were taken from literature [16]. The volume was partitioned into tetrahedral meshes ($\sim 10^4$ nodes), which were finer in the regions where the elastic energy was higher.

Misfit islands interact repulsively through their mutual strain fields in the substrate [17]. Their mutual interaction energy $\mathfrak{U}$ is the extra energy density needed to create an island in a certain location when another island already exists nearby and it is given by

$$\mathfrak{U}(\mathbf{r}) = U(\mathbf{r}) - U(\infty), \tag{2}$$

where $U(\mathbf{r})$ is the total strain energy (per unit volume) stored in the substrate and in the islands for the relative position of the island pair defined by $\mathbf{r} = (r_{[010]}, r_{[100]})$ [18] and $U(\infty)$ is the same quantity when $|\mathbf{r}|$ approaches infinity and no interactions exist between islands. The value of U is obtained by integrating the strain energy density $\rho = \frac{1}{2} C_{ijkl}(\varepsilon_{ij} - \varepsilon_0 \delta_{ij})(\varepsilon_{kl} - \varepsilon_0 \delta_{kl})$ over the island pair and the substrate and normalizing the result to the total island volume.

Figure 1(a) shows the interaction energy calculated for a pair of Ge domes grown on the flat Si(001) surface [the island shape is sketched in the inset of Fig. 2(a)]; the corresponding contour plot is reported in Fig. 1(b). The interaction potential reflects the fourfold symmetry of the island and results in an energetic barrier to island coalescence with local minima around the $\langle 001 \rangle$ directions. The shape of the interaction energy surface is strongly modified on the vicinal substrate [Figs. 1(c) and 1(d)]. The breaking of the island's symmetry induced by substrate vicinality produces directions along which islands can get into contact with low-elastic repulsion. Specifically, elastically soft configurations are achieved

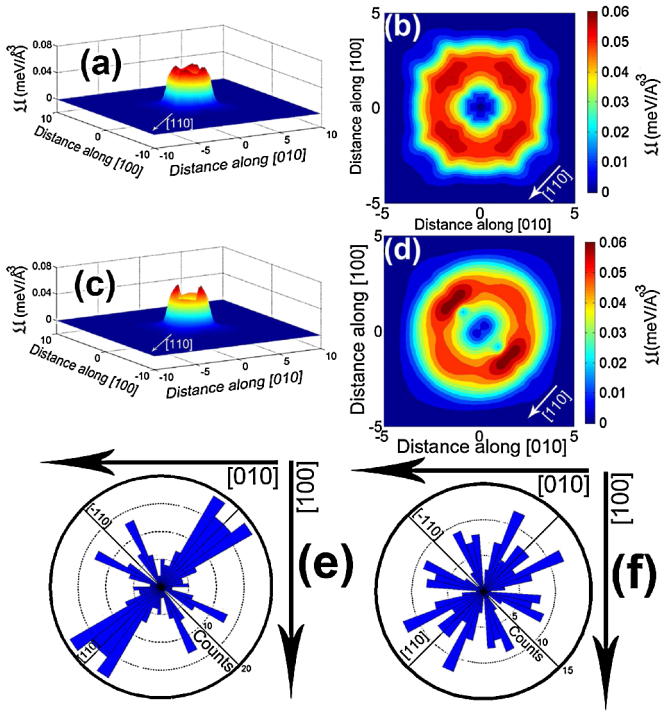

FIG. 1 (color online). (a) Interaction energy surface of Ge domes on the flat Si(001) surface and (b) corresponding contour plot. (c) Interaction energy surface of Ge domes on 10°-miscut Si(001) surface and (d) corresponding contour plot. Angular distribution of impingement directions measured (e) on 8°-miscut Si(001) substrates and (f) on 10°-miscut Si(001) substrates at 7.5 ML of Ge coverage.

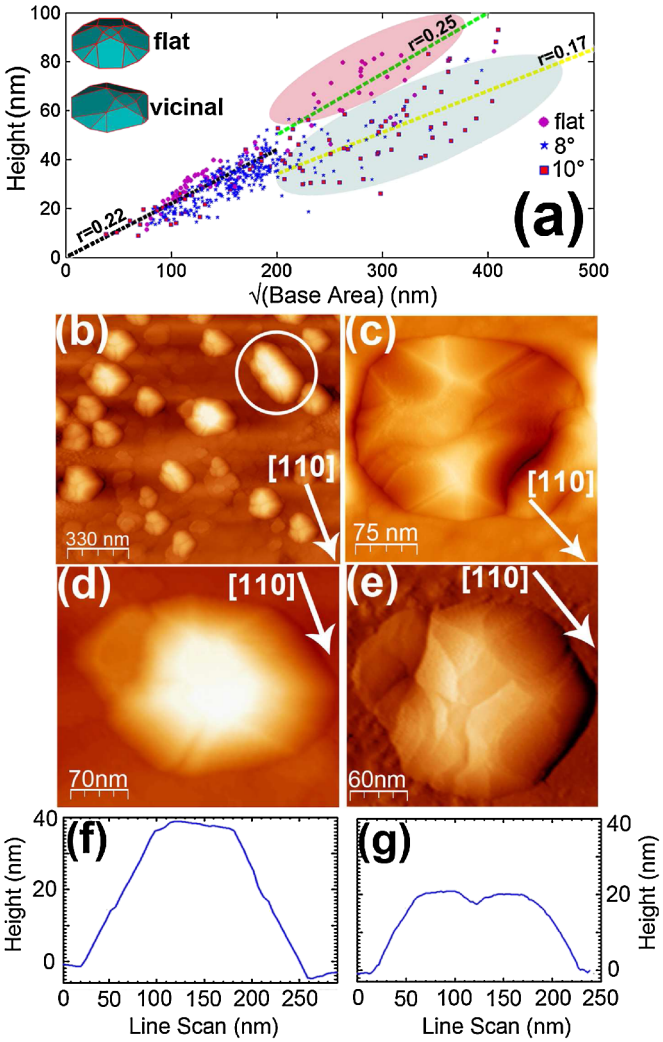

FIG. 2 (color online). (a) Shape evolution of Ge islands on flat (●), 8°-miscut (★), 10°-miscut (■) Si(001) surface. The dashed lines show the h/b linear dependence for different aspect ratios. In the inset, the morphology of the domes on flat and misoriented substrates is sketched. STM images at 7.5 ML of Ge coverage: (b) Ge superdomes on the flat Si(001) surface. A coalescence event is highlighted by a white circle. (c) Later stage of coalescence. Typical morphology of a superdome formed by (d) coarsening and (e) coalescence on the flat surface. Line scans along the [110] direction of superdomes formed (f) by coarsening and (g) by coalescence.

for islands interacting within an angular window of approximately $\pm 60°$ about the [110] miscut direction [Fig. 1(d)]. We now show that the observed change in the shape of elastic-interaction potential provides a chance for orienting the growth of Ge domes.

Ge films were grown by physical-vapor deposition on the singular Si(001) surface and on vicinal substrates misoriented by 8° and 10° towards the [110] direction at $T = 600\,°\mathrm{C}$ and at constant flux of 1.8×10^{-3} ML/s. Measurements were carried out *in situ* with a variable temperature scanning tunneling microscope (STM) under ultrahigh-vacuum conditions ($p < 3 \times 10^{-11}$ torr) [19].

Previous studies on the flat Si(001) surface have shown that Ge domes evolve into larger dislocated islands named "superdomes" [20,21]. The transition to superdomes is ruled either by anomalous coarsening or by coalescence [22,23]. A snapshot of the dome's coalescence can be seen in Fig. 2(b). As reported by Richard *et al.* [24], the two processes lead to different final morphologies, which can be easily distinguished in STM images. Superdomes formed by coalescence [Fig. 2(e)] have a plateaulike top and, thus, a significantly smaller aspect ratio than those resulting from coarsening [Fig. 2(d)]. This can be easily seen comparing the corresponding line scans through the middle of the islands [Figs. 2(g) and 2(f)]. Besides, in the case of coalescence, flat-top superdomes present a wedge-defect at the boundary among the impinged islands [25] [See Figs. 2(c), 2(e), and 2(g)]. By exploiting the morphological difference, it is possible to quantify the relative abundance of each type of superdome by means of a statistical analysis of island height-to-width ratio. In Fig. 2(a), the island height h is plotted as a function of the square root of the base area, i.e., the base width b. On the flat substrate, most of the Ge domes, which have an aspect ratio $r = h/b$ of 0.22 [26], evolve into steeper islands with r scattered around 0.25, a value consistent

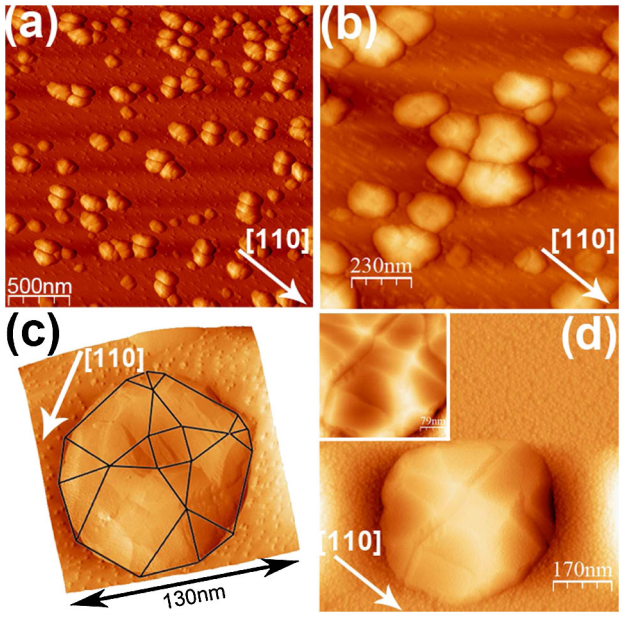

FIG. 3 (color online). STM images at 7.5 ML of Ge coverage: (a)–(b) Formation of Ge superdomes by coalescence on the 8°-miscut Si(001) surface. (c)–(d) Ge superdomes presenting the typical wedge defect after coalescence.

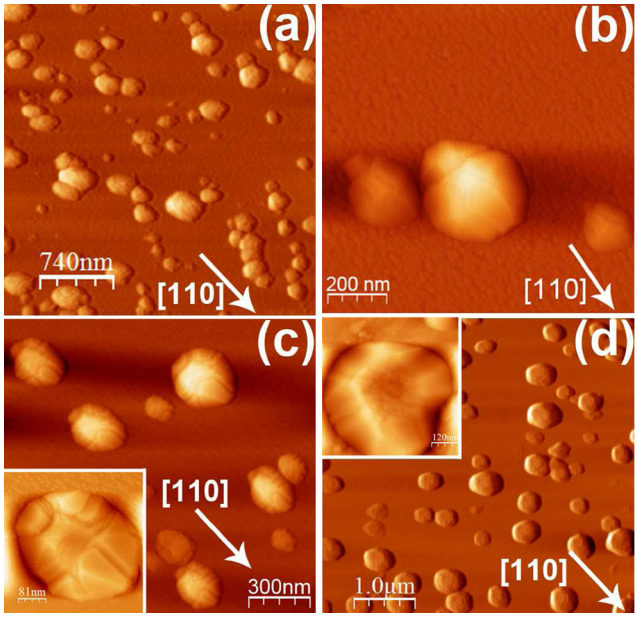

FIG. 4 (color online). STM images: (a)–(b) Formation of Ge superdomes by coalescence on the 10°-miscut Si(001) surface at 7.5 ML of Ge coverage. (c) Highly dislocated Ge islands after coalescence at 8 ML of Ge coverage. (d) Same sample of panel (c) after 30 min annealing at 720 °C: flat-top superdomes are formed.

with those of dislocated islands formed by coarsening [24]. Thus, in our experimental conditions, coarsening is the dominant pathway for superdome formation on the flat Si(001) surface.

We find that substrate misorientation is able to switch the growth evolution of Ge domes to the other possible path, promoting the dome's coalescence and, hence, the formation of flat-top superdomes. Concerning Fig. 2(a), the majority of islands grown on vicinal substrates evolve from domes ($r \approx 0.22$) toward shallow superdomes with aspect ratios around 0.17. Moreover, STM images clearly show that extensive coalescence occurs on 8° and 10°-miscut Si(001) surfaces [Figs. 3(a), 3(b), 4(a), and 4(b), respectively]. As aforementioned, a "grain boundary" is seen at the sites where coalescence has occurred [Figs. 3(c) and 3(d)]. We suggest that these grown-in defects directly mediate the formation of flat-top superdomes by promoting additional strain relief through the injection of stacking faults and threading dislocations during subsequent Ge overgrowth [27]. In fact, a high density of defects is observed when a further 0.5 ML of Ge is evaporated [Fig. 4(c)]. The flat-top morphology is finally achieved after 30 min annealing at $T = 720\,^{\circ}\mathrm{C}$ [Fig. 4(d)].

Figures 1(e) and 1(f) show angle histogram plots of the distribution of impingement directions of islands grown on highly misoriented substrates. Along the elastically soft directions around [110], the number of impingements is impressively higher, indicating that the elastic-interaction anisotropy is the main driving force for the observed changes in Ge growth evolution. Thus, the modified elastic interaction determines the transition between a coarsening-dominated growth to an extended coalescence regime in which the impingement directions are dictated by the shape of the elastic potential.

Finally, we emphasize that our analysis is readily applicable to other heteroepitaxial systems, such as InAs/GaAs, GaP/GaAs, etc., which have perspective applications in photonics [28] and quantum computation [29]. For all these systems, the elastic field is a common key parameter and, hence, its knowledge is of paramount importance for future technological advances.

In summary, we have used substrate vicinality to modulate the shape of the elastic-interaction potential between Ge nanostructures. The fourfold symmetry of elastic field is thereby reduced to twofold, producing directions of low elastic interaction. The modified elastic pattern orients Ge/Si heteroepitaxy towards an unusual pathway which is dominated by coalescence. A simple model based on continuum elasticity captures the essential of the experimental behavior.

We acknowledge the partial contribution of the Queensland Government through the NIRAP project "Solar Powered Nanosensors".

[1] B. Yang, F. Liu, and M. G. Lagally, Phys. Rev. Lett. **92**, 025502 (2004).

[2] N. Motta, P. Szkutnik, M. Tomellini, A. Sgarlata, M. Fanfoni, F. Patella, and A. Balzarotti, C.R. Physique **7**, 1046 (2006).

[3] P. Szkutnik, A. Sgarlata, N. Motta, E. Placidi, I. Berbezier, and A. Balzarotti, Surf. Sci. **601**, 2778 (2007).
[4] J. Tersoff, C. Teichert, and M. G. Lagally, Phys. Rev. Lett. **76**, 1675 (1996).
[5] F. Montalenti, A. Marzegalli, G. Capellini, M. D. Seta, and L. Miglio, J. Phys. Condens. Matter **19**, 225001 (2007).
[6] L. Persichetti, A. Sgarlata, M. Fanfoni, and A. Balzarotti, Phys. Rev. Lett. **104**, 036104 (2010).
[7] B. J. Spencer and J. Tersoff, Appl. Phys. Lett. **96**, 073114 (2010).
[8] L. Persichetti, A. Sgarlata, M. Fanfoni, and A. Balzarotti, Phys. Rev. B **82**, 121309(R) (2010).
[9] S. Christiansen, M. Albrecht, H. P. Strunk, and H. J. Maier, Appl. Phys. Lett. **64**, 3617 (1994).
[10] S. Noda, T. Abe, and M. Tamura, Phys. Rev. B **58**, 7181 (1998).
[11] J. Stangl, V. Holý, and G. Bauer, Rev. Mod. Phys. **76**, 725 (2004).
[12] B. Voigtländer, Surf. Sci. Rep. **43**, 127 (2001).
[13] I. Berbezier and A. Ronda, Surf. Sci. Rep. **64**, 47 (2009).
[14] G. Vastola, R. Gatti, A. Marzegalli, F. Montalenti, and L. Miglio, in *Self-Assembled Quantum Dots*, edited by Z. M. Wang (Springer, New York, NY, 2008), Vol. 1, Chap. 14, pp. 421–438.
[15] Since recent experimental studies have shown that cylindrical symmetry describes the composition profile of domes at the typical temperature of Ge growth, intermixing will likely result in a rigid rescaling of the interaction energy. Using linear interpolation for the elastic constants and the initial strain ϵ_0 for $Si_{0.5}Ge_{0.5}$ domes, we estimated that the scaling factor corresponds to 1.5 in units of base width b.
[16] F. Schäffler, in *Properties of Advanced Semiconductor Materials*, edited by M. E. Levinshtein, S. L. Rumyantsev, and M. S. Shur (John Wiley & Sons, Inc., New York, 2001), pp. 149–188.
[17] H. T. Johnson and L. B. Freund, J. Appl. Phys. **81**, 6081 (1997).
[18] The island separation is normalized to the island size.
[19] P. D. Szkutnik, A. Sgarlata, S. Nufris, N. Motta, and A. Balzarotti, Phys. Rev. B **69**, 201309 (2004).
[20] T. I. Kamins, G. M. Ribeiro, D. A. A. Ohlberg, and R. S. Williams, J. Appl. Phys. **85**, 1159 (1999).
[21] A. Rastelli and H. von Känel, Surf. Sci. **515**, L493 (2002).
[22] T. Merdzhanova, S. Kiravittaya, A. Rastelli, M. Stoffel, U. Denker, and O. G. Schmidt, Phys. Rev. Lett. **96**, 226103 (2006).
[23] M. I. Richard, T. U. Schülli, G. Renaud, E. Wintersberger, G. Chen, G. Bauer, and V. Holý, Phys. Rev. B **80**, 045313 (2009).
[24] M. I. Richard, G. Chen, T. U. Schülli, G. Renaud, and G. Bauer, Surf. Sci. **602**, 2157 (2008).
[25] A. Sakai and T. Tatsumi, Phys. Rev. Lett. **71**, 4007 (1993).
[26] M. Stoffel, A. Rastelli, J. Tersoff, T. Merdzhanova, and O. G. Schmidt, Phys. Rev. B **74**, 155326 (2006).
[27] F. K. LeGoues, M. Copel, and R. M. Tromp, Phys. Rev. B **42**, 11 690 (1990).
[28] A. J. Shields, Nat. Photon. **1**, 215 (2007).
[29] *The Physics of Quantum Information*, edited by D. Bouwmeester, A. Eckert, and A. Zeilinger (Springer, Heidelberg, 2000).